The Astrophysical Journal, 655:345–350, 2007 January 20


# HOW HOT IS THE WIND FROM TW HYDRAE?[1]

Christopher M. Johns-Krull
Department of Physics and Astronomy, Rice University, Houston, TX; cmj@rice.edu

and

Gregory J. Herczeg
California Institute of Technology, Pasadena, CA; gregoryh@astro.caltech.edu
*Received 2006 July 25; accepted 2006 August 30*

## ABSTRACT

It has recently been suggested that the winds from classical T Tauri stars in general, and the wind from TW Hya in particular, reaches temperatures of 300,000 K while maintaining a mass-loss rate of $\sim 10^{-11}\ M_{\odot}\ \mathrm{yr}^{-1}$ or larger. If confirmed, this would place strong new requirements on wind launching and heating models. We therefore reexamine spectra from the Space Telescope Imaging Spectrograph aboard the *Hubble Space Telescope* and spectra from the *Far Ultraviolet Spectroscopic Explorer* satellite in an effort to better constrain the maximum temperature in the wind of TW Hya. We find clear evidence for a wind in the C II doublet at 1037 Å and in the C II multiplet at 1335 Å. We find no wind absorption in the C IV $\lambda$1550 doublet observed at the same time as the C II $\lambda$1335 line or in observations of O VI observed simultaneously with the C II $\lambda$1037 line. The presence or absence of C III wind absorption is ambiguous. The clear lack of a wind in the C IV line argues that the wind from TW Hya does not reach the 100,000 K characteristic formation temperature of this line. We therefore argue that the available evidence suggests that the wind from TW Hya, and perhaps all classical T Tauri stars, reaches a maximum temperature in the range of 10,000–30,000 K.

*Subject headings:* accretion, accretion disks — stars: individual (TW Hydrae) — stars: mass loss — stars: pre–main-sequence

## 1. INTRODUCTION

Mass loss in the form of a wide-angle wind and/or collimated jet is a common feature observed in young, low-mass stars that are still surrounded by accretion disks (for a review see Bally et al. 2007). The material in these disks eventually accretes onto the central star, gets ejected in an outflow, or is incorporated into planets or other solar system–like bodies. Understanding the processes through which young stars interact with and eventually disperse their disks is critical for understanding the rotational evolution of stars and the formation of planets. Mass loss appears to be a necessary component in the accretion process both observationally as mentioned above and theoretically: angular momentum must be carried away in order to allow disk and stellar accretion to occur, and magnetized winds are efficient at removing angular momentum (e.g., Pudritz et al. 1991; Shu et al. 1994).

Signatures of mass loss are observed primarily in optical, infrared, and radio wavelength spectral diagnostics. Bipolar outflows are observed in millimeter wavelength CO lines and other molecular tracers in the millimeter and submillimeter range (e.g., see review by Arce et al. 2007). In the infrared, emission in $H_2$ (e.g., Gueth & Guilloteau 1999; Stanke et al. 2002) and [Fe II] (e.g., Reipurth et al. 2000) lines are regularly seen in outflows from young stars. At optical wavelengths, Herbig-Haro (HH) objects and their associated stellar jets are routinely imaged in narrowband filters centered on H$\alpha$ or on a host of forbidden lines. High-resolution images of the central engine show that these jets originate from young stars surrounded by circumstellar disks, with the jet usually emerging perpendicular to the disk like that clearly seen in the case of HH 30 (Burrows et al. 1996; Ray et al. 1996). Spectroscopically, winds and jets are diagnosed by the appearance of P Cygni–like line profiles in permitted lines, such as H$\alpha$ (and other Balmer lines) and Na D (e.g., Mundt 1984; Reipurth et al. 1996; Alencar & Basri 2000), and in the profiles of forbidden lines, which often show a strong asymmetry with substantial blueshifted emission with little or no redshifted emission (e.g., Edwards et al. 1987; Hamann 1994). More recently, jets and winds from classical T Tauri stars (CTTSs) have been detected at shorter wavelengths corresponding to higher temperature emissions. Hartigan et al. (1999) detect several ultraviolet (UV) Fe II emission lines in the HH 47A bow shock, and several irradiated jets with UV signatures have been discovered recently (e.g., Reipurth et al. 1998; Bally & Reipurth 2001). Gomez de Castro & Verdugo (2001) identify a feature in the UV semiforbidden emission lines of C III] $\lambda$1908 and Si III] $\lambda$1892 that they associate with shocks at the base of the jet in a few CTTSs. At X-ray energies, a number of jets have also recently been detected (e.g., Pravdo et al. 2001; Favata et al. 2002; Bally et al. 2003). This X-ray emission forms in the fastest shocks associated with these stellar jets (see also Bally et al. 2007). While these high-excitation emissions appear to be associated with shocks within the jets from young stars, until recently it was generally thought that the stellar or disk wind at the base of these jets was only heated to a level that could produce features such as the P Cygni–like profiles visible in the Balmer lines.

A hot wind component, possibly with an origin on the star as opposed to in the disk, has recently been proposed by a few authors. Beristain et al. (2001) argue for a hot wind component in CTTSs based on the analysis of high-resolution He I and He II line profiles observed in the optical. Takami et al. (2002) and Edwards et al. (2003) find obvious blueshifted absorption below

[1] This work is based on observations with the NASA/ESA *Hubble Space Telescope*, obtained at the Space Telescope Science Institute, which is operated by the Association of Universities for Research in Astronomy, Inc., under NASA contract NAS5-26555. These observations are associated with program GTO-7718. This work is also based on observations made with the NASA/CNES/CSA *Far Ultraviolet Spectroscopic Explorer*, which is operated for NASA by the Johns Hopkins University under NASA contract NAS5-32985.

the local continuum in the He I $\lambda$10830 line in six young, low-mass stars, again providing evidence for a hot wind component forming relatively near the star. Edwards et al. (2003) point out that the strength and ubiquity of this absorption indicates that the wind emanates over a large solid angle from the star: the He I $\lambda$10830 line does not trace a highly collimated flow. These results are reinforced by Edwards et al. (2006), who find subcontinuum He I $\lambda$10830 wind absorption in 26 of 38 CTTSs. The 5876 and 10830 Å lines of He I require a strong ionizing flux or a high temperature for excitation, as their upper states lie $\sim$20 eV above the ground level. If these lines are primarily collisionally excited, temperatures of $\sim$25,000 K are required to excite them (Athay 1965; Avrett et al. 1976). With photoionization followed by recombination and cascade, helium excitation can take place at local kinetic temperatures between 8000 and 15,000 K (Zirin 1975; Heasley et al. 1974; Wahlstrom & Carlsson 1994). CTTSs in general (e.g., Feigelson et al. 2002), and TW Hya in particular (Kastner et al. 2002), are strong X-ray sources, so the detection of these He I lines in CTTS winds still leaves a wide range of possible temperatures present in these outflows. Dupree et al. (2005) detect He I $\lambda$10830 absorption in the wind from TW Hya and T Tau. They combine these observations with an analysis of the line profiles of C III $\lambda$977 and O VI $\lambda$1032 observed with the *Far Ultraviolet Spectroscopic Explorer* (*FUSE*) satellite to suggest that CTTSs possess continuous, smoothly accelerating winds that reach velocities of $\sim$400 km s$^{-1}$ and temperatures of $\sim$300,000 K. These results are based primarily on the *FUSE* data for TW Hya, since the data for T Tau are much lower in quality. Dupree et al. (2005) find a minimum mass-loss rate for the O VI line of $2.3 \times 10^{-11}\ M_{\odot}\ \mathrm{yr}^{-1}$.

Such a hot temperature for the wind from TW Hya is surprising, particularly given the high mass-loss rate. Alencar & Batalha (2002) and Herczeg et al. (2004) estimate a mass accretion rate onto TW Hya of $\sim 2 \times 10^{-9}\ M_{\odot}\ \mathrm{yr}^{-1}$. Most estimates suggest that the mass-loss rate from CTTSs is 0.1–0.3 times that of the mass accretion rate (Königl & Pudritz 2000; Shu et al. 1994), implying that the mass-loss rate from TW Hya may be as high as $5 \times 10^{-10}\ M_{\odot}\ \mathrm{yr}^{-1}$. A wind with such a high temperature and high mass-loss rate puts strong constraints on the ultimate origin and heating of winds from CTTSs. Current theories of mass loss from CTTSs primarily produce cold, magnetocentrifugally driven flows from the disks around these stars (e.g., Königl & Pudritz 2000; Shu et al. 2000) that are then heated by a combination of ambipolar diffusion and X-rays to temperatures of $\sim 10^4$ K (Shang et al. 2002, 2007). Photoevaporation of the surface layer of the disk may also produce a low-velocity ($\sim$10 km s$^{-1}$) wind with a characteristic temperature of $10^4$ K as well (e.g., Matsuyama et al. 2003; Font et al. 2004). Thus, if the Dupree et al. (2005) suggestion holds true, a totally new heating, and possibly driving, mechanism must be identified. The analysis presented by Dupree et al. (2005) relies on the asymmetric *shape* of the line profiles tracing the hot gas: no true absorption against a local continuum is detected. Therefore, we reexamine the published (Herczeg et al. 2002, 2004; Dupree et al. 2005) high-resolution spectra from the Space Telescope Imaging Spectrograph (STIS) aboard the *Hubble Space Telescope* (*HST*) and from the *FUSE* satellite to look for firm wind signatures and confirm the high proposed temperature in the wind of TW Hya. The STIS and *FUSE* bandpasses cover several lines with characteristic formation temperatures ranging from $\sim 10^4$ to $\sim$300,000 K. We find firm evidence against the proposed wind in the C IV and O VI lines of TW Hya. We therefore conclude that the wind in fact does not reach (at least at large optical depth as claimed) a temperature of $\sim$100,000 K, characteristic of the formation of the C IV line. In § 2 we describe the observational data. Section 3 presents our analysis, and § 4 gives a discussion of our results.

## 2. OBSERVATIONS AND DATA REDUCTION

We observed TW Hya with the E140M echelle grating and the $0.5'' \times 0.5''$ aperture on *HST* STIS for 2.3 ks as part of *HST* program GTO-7718. The spectrum spans from 1170 to 1700 Å with $R = 25{,}000$. The data were reduced using the standard CALSTIS reduction package written for IDL. The flux calibration is accurate to $\sim$10%. The wavelength calibration is accurate to $\sim$5 km s$^{-1}$. This spectrum was described by Herczeg et al. (2002).

We also observed TW Hya with the LWRS ($30''$) aperture on *FUSE* for 2 ks on 2000 June 3 for program GTO-P186 and for 30.25 ks on 2003 February 20–21 for program GTO-P186. Each visit includes several separate integrations. *FUSE* consists of four co-aligned telescopes, each of which has two channels coated with LiF and SiC (Moos et al. 2000). Each observation yields eight independent spectra covering $\sim$90 Å.

We reduced the *FUSE* spectra using version 3.1.3 of the CalFUSE standard data reduction pipeline.[2] We combined each integration using the `idf_combine` routine and subsequently extracted the counts in the spectrum and in the background. Pulse-height values for each LiF and SiC spectrum were restricted to those detected in the individual extraction windows to reduce background noise. We use the standard CalFUSE wavelength solution; however, the zero point for this solution is not correct and must be fixed using the observed spectrum. For our 30 ks visit, we calibrated wavelengths at $\lambda > 1000$ Å using 25 different $H_2$ lines in this region, setting the wavelength zero point so that these lines appear at the radial velocity of the star (Herczeg et al. 2002). We calibrated the zero point of wavelengths at $\lambda <$ 1000 Å by cross-correlating the emission profiles for the N III $\lambda$991.5 lines and several O I airglow lines, which appear in both the longer (calibrated with the $H_2$ lines) and shorter wavelength channels that overlap between 985 and 1005 Å. We calibrated the wavelengths of our 2 ks exposure by cross-correlating the spectra in regions with strong lines. We then summed the counts, background, and effective area in each spectrum to obtain a single spectrum.

Our final spectrum spans from 905 to 1187 Å with $R \sim$ 15,000. The error in our wavelength solution is $\sim$10 km s$^{-1}$ at $\lambda > 1000$ Å and $\sim$15 km s$^{-1}$ at $\lambda < 1000$ Å. The absolute and relative flux calibration is accurate to $\sim$10% and $\sim$5%, respectively, at wavelengths discussed in this paper. The background subtraction is accurate to $(0.5\text{–}3) \times 10^{-15}$ ergs cm$^{-2}$ s$^{-1}$ Å$^{-1}$. To reduce possible contamination by airglow lines, we restrict our analysis to data obtained during *FUSE* nighttime.

## 3. ANALYSIS

### 3.1. *Wind Absorption of* $H_2$ *and below the Local Continuum*

Dupree et al. (2005) assert the presence of a hot ($\sim$300,000 K) wind from TW Hya based on the *shape* of the O VI and C III emission-line profiles. When considering the shape of emission lines, there can be an ambiguity between self-absorption in some part of the line profile and simply a lack of emission in this same part of the profile. The presence of a wind is much more firmly deduced when absorption is detected against a local continuum. Contrary to the statements in Dupree et al. (2005), a UV continuum is detected from TW Hya, as is evident in many of the figures shown Herczeg et al. (2002) based on STIS data. This continuum

[2] See http://fuse.pha.jhu.edu/analysis/calfuse.html.

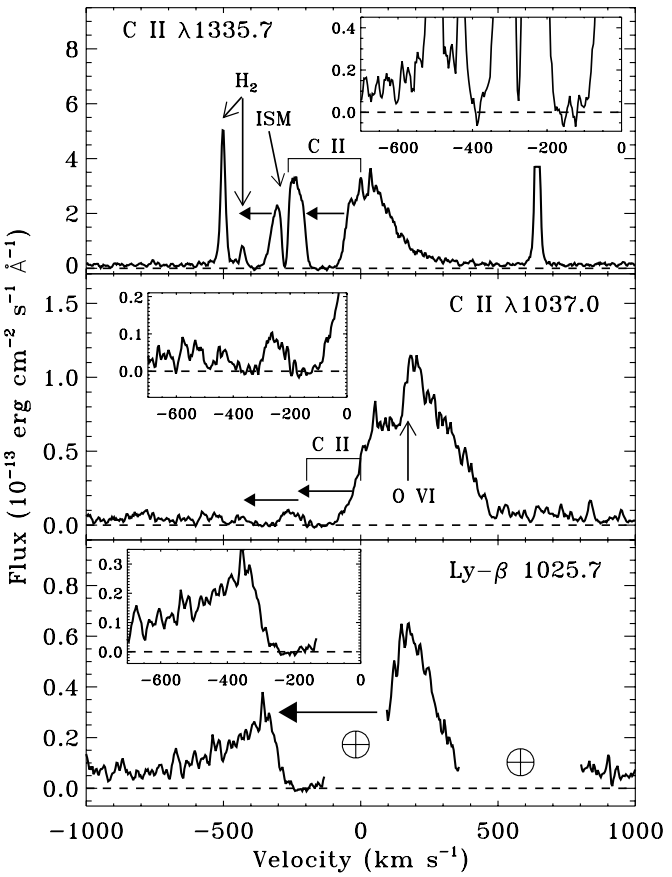


FIG. 1.—Line profiles of UV emission lines in TW Hya that show blueshifted wind absorption below the local continuum. The C II $\lambda$1335 lines in the top panel come from the STIS spectrum. The middle and bottom panels show C II $\lambda$1037, O VI $\lambda$1038, and Ly$\beta$ in TW Hya observed by *FUSE*. The dashed horizontal line marks the zero-flux level. Horizontal arrows indicate the range over which wind absorption is detected. The inserts clearly show this wind absorption below the local continuum in each line.

is clearly visible in Figures 1 and 3. Also evident in Figure 1 is that the flux goes to zero in blueshifted wind absorption profiles for key lines from both the STIS and *FUSE* spectra.

All of the strong, unblended, relatively low temperature lines present in the STIS spectrum of TW Hya, including the C II $\lambda$1335 lines, the O I $\lambda$1305 triplet, and the Si II doublets at 1260 and 1530 Å, show evidence for wind absorption below the local continuum. In the top panel of Figure 1, we show that the wind absorption from the stronger, red members of the C II $\lambda$1335 lines[3] stays at zero flux out to a velocity of $\sim -185$ km s$^{-1}$ and that the flux in the wind of the weaker blue member stays at zero flux out to a velocity of $-165$ km s$^{-1}$. The middle and bottom panels show line profiles from the *FUSE* spectrum of TW Hya that show clear absorption below the local continuum. The middle panel shows the C II $\lambda$1037 doublet, which is blended with the O VI $\lambda$1038 line. Absorption below the local continuum is detected in this C II doublet and in H I Ly$\beta$, which are both adjacent to the O VI lines. The blue member of both the C II $\lambda$1037 doublet and the C II $\lambda$1335 multiplet suffers wind absorption by the red members (see also § 3.2). To quantify the above, we present in Table 1 continuum measurements near each of the lines of interest discussed here. The continuum in each region is detected at a very significant level, whereas in the wind absorption region of C II $\lambda$1335.7, for example, the measured flux is $(1.2 \pm 0.7) \times 10^{-15}$ ergs cm$^{-2}$ s$^{-1}$ Å$^{-1}$ in the velocity range $-90$ to $-170$ km s$^{-1}$.

[3] We note that the C II $\lambda$1335 feature is a triplet with lines at 1334.532, 1335.663, and 1335.708 Å; however, the middle member of this triplet should be quite weak due to its low oscillator strength, which is approximately an order of magnitude lower than that of the 1335.708 Å line (Kurucz & Bell 1995). Therefore, in Fig. 1 we mark only the positions of the bluemost and redmost members of the multiplet.

TABLE 1
CONTINUUM MEASUREMENTS NEAR POTENTIAL WIND ABSORPTION FEATURES

| Line | Continuum Regions[a] (Å) | Continuum Flux[b] |
|---|---|---|
| C III $\lambda$977.0 | 973–975.5, 979–983.5 | 2.7 ± 0.4 |
| H I Ly$\beta$ $\lambda$1025.7 | 1018–1023, 1029.6–1030.7 | 5.0 ± 0.2 |
| O VI $\lambda$1031.9 | 1029.6–1030.7, 1034.5–1035.5 | 5.0 ± 0.3 |
| C II $\lambda$1037.0 | 1034.5–1035.5, 1042–1046.3 | 3.2 ± 0.2 |
| O VI $\lambda$1037.6 | 1034.5–1035.5, 1042–1046.3 | 3.2 ± 0.2 |
| C II $\lambda$1335.0 | 1330–1333, 1339–1342 | 11.8 ± 0.4 |
| C IV $\lambda$1549.0 | 1544.5–1546 | 23.8 ± 1.0 |

[a] Regions used to estimate the continuum flux at the respective emission line.
[b] Units are $10^{-15}$ ergs cm$^{-2}$ s$^{-1}$ Å$^{-1}$.

The top panel of Figure 1 also shows that the $H_2$ 1333.797 Å line is located at $-165$ km s$^{-1}$ from the C II $\lambda$1334.5 line, within the wind absorption. (Again, the red member of the multiplet shows that the wind absorption in these lines is strong out to at least $-185$ km s$^{-1}$.) Of 140 $H_2$ line fluxes from TW Hya modeled by Herczeg et al. (2004), this $H_2$ line is conspicuous in that it is the only line that is not well fit. The observed flux of 7.9 ± 0.7 ergs cm$^{-2}$ s$^{-1}$ in this line is a factor of 6 below its predicted level. Herczeg et al. (2002) determine that the UV $H_2$ emission lines originate in the disk within 2 AU of the star, and Figure 1 shows that the $H_2$ emission is subject to wind absorption.

### 3.2. *The Proposed Hot Wind*

Dupree et al. (2005) diagnose the presence of a hot wind from TW Hya by examining the shape of the C III $\lambda$977 and O VI $\lambda$1032 emission lines. These lines display an asymmetry in their profiles such that there is more emission on the red side of the profile than on the blue. This could represent self-absorption or scattering in a wind, or an accretion flow that preferentially produces redshifted emission. We show these and the C IV $\lambda$1548 line profiles in Figure 2. Also shown is a Gaussian fit to the right side of the line profile, as was done by Dupree et al. (2005). The Gaussian fit is centered at 0 km s$^{-1}$, and its width and amplitude are fit to the red wing of the emission-line profile. The red side of the C III and O VI are fairly Gaussian in shape. The C IV line is not well fit by a Gaussian, but the fitting illustrates the essential points discussed by Dupree et al. (2005). They cite the flux deficit on the blue side of the profile relative to the Gaussian fit as evidence for the hot wind. Dupree et al. (2005) then estimate the maximum velocity in the wind traced by the different diagnostics by estimating where the fit rejoins the observations in the far blue wing. For our data reductions and fits, we find velocities of $\sim -275$, $\sim -400$, and $\sim -400$ km s$^{-1}$ for C III, O VI, and C IV, respectively, which are similar to the values of $-325$ and $-440$ km s$^{-1}$ for C III and O VI, respectively, found by Dupree et al. (2005).

### 3.3. *A Closer Look at the STIS* C IV *and* C II *Lines*

The C IV $\lambda$1550 doublet provides three very significant clues that clearly show that there is no wind absorption in these lines. First, the profile on the blue side of the C IV does not go below the local continuum (i.e., to a flux of zero) as is the case for the wind

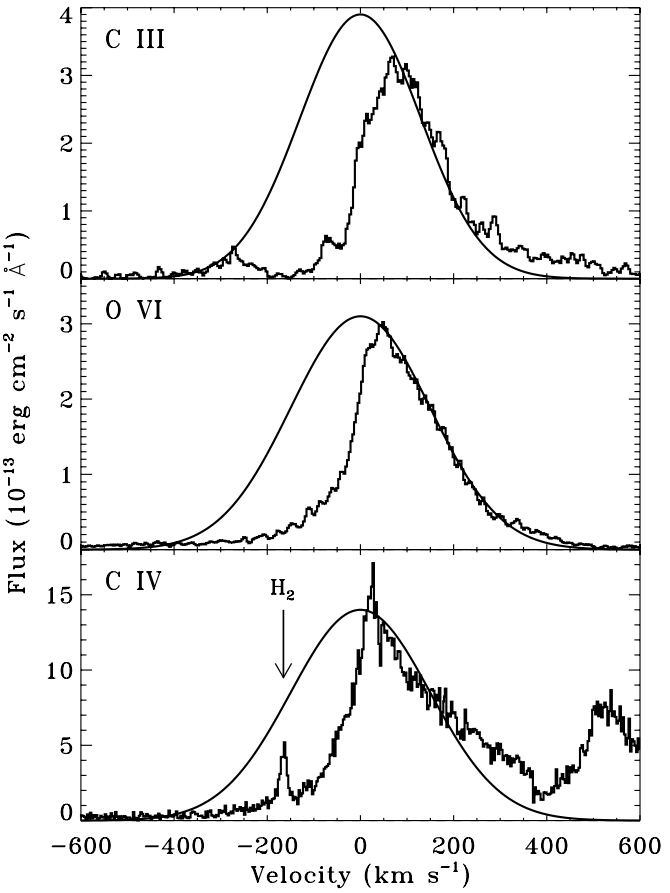


FIG. 2.—Line profiles of C III $\lambda$977, O VI $\lambda$1032, and C IV $\lambda$1548. Shown with each line is a Gaussian fit to the red side of the profile.

absorption lines shown in Figure 1. One may counter that the optical depth in the C IV lines is simply lower than in the lines shown in Figure 1. The additional points address this concern.

An $H_2$ line at 1547.4 Å is located at a velocity of $-165$ km s$^{-1}$ relative to C IV $\lambda$1548, which is well within any possible wind absorption due to C IV. This $H_2$ line has a measured flux of $(35.3 \pm 2.7) \times 10^{-15}$ ergs cm$^{-2}$ s$^{-1}$ and a predicted flux of $33.0 \times 10^{-15}$ ergs cm$^{-2}$ s$^{-1}$ (Herczeg et al. 2004). The blue wing of the C IV $\lambda$1548.19 line in the immediate vicinity of the 1547 Å $H_2$ line is reduced by a factor of $\sim$5.5 relative to the Gaussian fit at this velocity. Dupree et al. (2005) interpret this as wind absorption in the C IV line. The discussion in § 3.1 above demonstrates that the $H_2$ lines form inside the wind and will suffer absorption if a wind absorber overlaps a given $H_2$ line in wavelength. As a result, we would expect the 1547 Å $H_2$ line to have an observed flux about a factor of $\sim$5.5 below that predicted by Herczeg et al. (2004), as is in fact seen for the 1334 Å $H_2$ line shortward of C II $\lambda$1334.5 (see § 3.1). Since absolutely no absorption is detected in the 1547 Å $H_2$ line, we conclude that there is no significant wind absorption in C IV.

The third strike against a hot wind visible in the C IV lines is illustrated in Figure 3. Shown in black is the line profile for the blue components of the C II $\lambda$1335 (*top*) and the C IV (*middle*) lines. Shown in red is the red component of the respective lines overlaid and scaled to match near the peaks and in the blue wings. The two components of the C IV line have almost identical shapes, which is somewhat expected, since they trace almost exactly the same material. The red wing of the 1548.19 Å line extends to $\sim -130$ km s$^{-1}$ relative to the 1550.77 Å line, where any wind absorption due to the 1550.77 Å line should be quite strong. The bottom panel of Figure 2 shows that the observed flux in the 1548.19 Å line is down by a factor of $\sim$5.5 at this velocity. The red wing of the 1548.19 Å line shows no such evidence for absorption due to the "wind" traced by the 1550.77 Å line.

This is not at all the case for C II, where we know there truly is a wind present. By overplotting the C II lines in the top panel of Figure 3, we see that the short-wavelength (1334.53 Å) member of the multiplet shows dramatic absorption due to the wind from the long-wavelength members of the multiplet. The different members of the multiplet trace essentially the same material. The red profile in the top panel of Figure 3 shows that the emission in these lines should extend to $\sim$+300 km s$^{-1}$; however, the 1334.53 Å line only extends to $\sim$+80 km s$^{-1}$ because of the strong wind absorption due to the red members of the multiplet.

If these C IV lines (absorption and emission components) form in a wind, the far red wings are formed by material on the far side of the star. TW Hya has a large inner hole in its disk (e.g., Johns-Krull & Valenti 2001), so this material would be visible. If the emission component of the line forms in the magnetospheric accretion flow, then it forms very near the star. Regardless of whether the emission is produced by the accretion flow or the wind, the light would pass through the wind on the near side of TW Hya and should suffer absorption at any wavelength where the projected velocities from the two lines overlap. The total lack of detectable C IV absorption again leads us to conclude there is no significant amount of C IV in the wind from TW Hya.

### 3.4. *A Closer Look at the FUSE* O VI *and* C III *Lines*

The O VI emission-line profiles are similar to the C IV profiles, with strong redshifted emission extending to $\sim$+400 km s$^{-1}$ and much weaker blueshifted emission. The middle panel of Figure 1 demonstrates that the continuum flux goes to zero in wind absorption due to the nearby C II $\lambda$1037 doublet and the Ly$\beta$ 1025.7 Å line. However, Figures 2 and 3 demonstrate that we do not detect any subcontinuum absorption produced by the stronger member of the O VI doublet, at 1031.91 Å.

The long-wavelength member of the C II $\lambda$1037 doublet occurs at $-172$ km s$^{-1}$ relative to the O VI $\lambda$1037.6 line. The bottom panel of Figure 3 overlays two O VI lines, and the scaled C II $\lambda$1335.7 is used as an approximation for the C II $\lambda$1037.0 line profile. Any wind in the O VI $\lambda$1037.6 line would absorb most of the C II $\lambda$1037.0 line, but the red side of the C II line is strong, showing no indication of absorption. We therefore find an absence of any detectable O VI in the wind.

Whether the C III line shows wind absorption is ambiguous. The sensitivity of *FUSE* at 977 Å is lower than at 1035 Å, so the continuum is not as well detected. The continuum level measured between $-100$ and $-200$ km s$^{-1}$ from line center is $6 \times 10^{-15}$ ergs cm$^{-2}$ s$^{-1}$ Å$^{-1}$, which is higher than the local continuum of $2.7 \times 10^{-15}$ ergs cm$^{-2}$ s$^{-1}$ Å$^{-1}$. No definite C III wind absorption is detected, but we also cannot rule out some wind absorption that is either optically thin or narrower than that seen in other wind absorption lines. The nondetection is therefore ambiguous.

Some emission is present at $-270$ km s$^{-1}$, with a flux of 10% of that at the peak of the line profile. The flux in the C IV and O VI lines drops to 10% of the peak value at $-150$ km s$^{-1}$, while the C II lines show no emission shortward of $-200$ km s$^{-1}$. Therefore, the emission at $-270$ km s$^{-1}$ is probably not C III emission. An $H_2$ line at 976.2 Å may contribute as much as half of the flux at $-270$ km s$^{-1}$. We are unable to identify the additional emission as either airglow or other atomic lines. However, we are

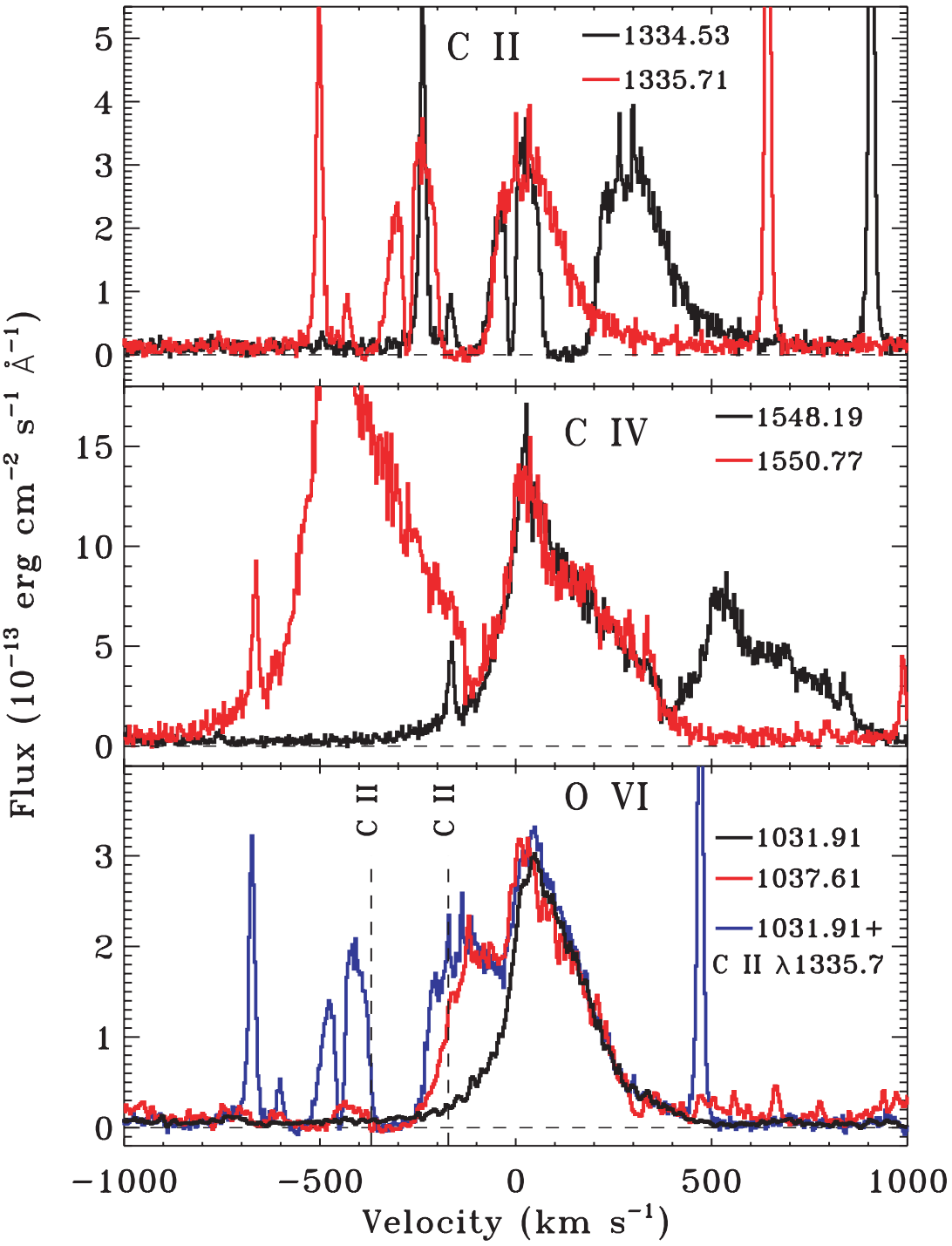


FIG. 3.—Line profiles of C II $\lambda$1335, C IV $\lambda$1550, and O VI $\lambda$1035. The black line shows the blue member of each multiplet. The red line shows the red member of each multiplet scaled to match the peak and blue wing of the blue member. The dashed horizontal line marks the zero-flux level. In the bottom panel, the blue line shows C II emission, scaled from the C II $\lambda$1335.7 line, added to the scaled O VI $\lambda$1032 line to estimate the profile of the C II $\lambda$1037 line.

unable to use the presence of emission at $-270$ km s$^{-1}$ to infer the presence of C III wind absorption.

## 4. DISCUSSION

The hot far-UV (FUV) emission lines from CTTSs are related to accretion, as is seen in correlations with mass accretion rate (Johns-Krull et al. 2000; Calvet et al. 2004). The line profiles are often complex and can show significant excess redshifted emission. Such an asymmetric line profile is naturally expected for optically thin lines that are produced by hot gas in downflowing accretion columns. Dupree et al. (2005) also suggest that narrow O VI profiles in the lower quality spectrum of T Tau could suggest wind absorption, but the narrow width is instead caused by strong absorption in interstellar $H_2$ lines (e.g., Roberge et al. 2001; Walter et al. 2003). However, asymmetric or narrow profiles of warm emission lines, including C II–C IV, O VI, He II, N V, and Si IV, are insufficient to infer the presence of a wind from CTTSs. Detecting wind absorption from FUV spectra of CTTSs requires measuring either subcontinuum absorption or absorption of nearby atomic or $H_2$ lines.

We conclusively find that no C IV wind absorption is detected in the STIS spectrum of TW Hya, based on several independent diagnostics. Since C IV and O VI trace gas at $T = 100{,}000$ and 300,000 K, respectively, the lack of any detectable C IV in the wind means that no higher temperature O VI gas will be detectable. We confirm this conclusion by finding an absence of O VI wind absorption in the *FUSE* spectrum of TW Hya. These findings emphasize the result that asymmetric line profiles with more red emission than blue as shown here do not necessarily diagnose the presence of a wind. Indeed, Lamzin et al. (2004) argue that the extended blue wings of C III $\lambda$977, C IV $\lambda$1550, and O VI $\lambda$1032 arise in the magnetospheric infall around TW Hya.

The lack of detectable absorption by C IV and the positive detection of C II wind absorption indicates that the abundance of C IV in the wind is less than 1% of that of C II. Based on the ionization equilibrium of C, this upper limit suggests a maximum wind temperature of <50,000 K. The detection of optically thin wind absorption in the He I $\lambda$10830 requires either some photoionization or temperatures of >25,000 K in the wind. In either case, some C III wind absorption is expected. Unfortunately the *FUSE* spectrum of TW Hya at 977 Å is not of high enough quality to clearly detect the presence or absence of C III in the wind.

In addition to C II and H I discussed above, wind absorption from TW Hya is detected in Al II, Si II, Mg II, O I, and N I but is not detected in C I or Si I. Wind absorption is also prevalent from the CTTS RU Lup (Herczeg et al. 2005), which has a much higher mass accretion rate than does TW Hya and therefore presumably a higher wind mass-loss rate. We observe the same wind absorption lines as seen in TW Hya, but the higher optical depth in the wind from RU Lup also allows us to detect Cl I, many Fe II lines, and Si III. The similarity in wind absorption lines from RU Lup and TW Hya suggests that the ionization of the wind can be similar for stars with mass-loss rates that likely differ by at least a factor of 10.

The absence of C I absorption in the wind of both TW Hya and RU Lup suggests that the temperature of the wind is >20,000 K. However, the presence of O I, Cl I, and Fe II in the wind requires gas at $T < 20{,}000$ K. We therefore speculate that the winds from CTTSs have a kinetic temperature of $\sim$10,000 K and that the ionization state is dominated by photoionization. Elements with first ionization potential longward of the Lyman limit are photoionized. A smaller amount of ionizing photons may also irradiate the wind, which would explain prevalent wind absorption in the He I recombination line at 10830 Å (Edwards et al. 2006), N I lines with lower levels excited to 2.4 eV, and the detection of Si III in the wind of RU Lup (Herczeg et al. 2005). No strong lines occur between 912 and 954 Å, which may explain why Cl I is not ionized in the wind of RU Lup.

We would like to acknowledge several useful comments from an anonymous referee. C. M. J.-K. acknowledges partial support through program AR-9933 provided by NASA through a grant from the Space Telescope Science Institute, which is operated by the Association of Universities for Research in Astronomy, Inc., under NASA contract NAS5-26555. G. J. H. acknowledges partial support from *FUSE* program GO-C067, provided by NASA contract NAS5-32985.

## REFERENCES

Alencar, S. H. P., & Basri, G. 2000, AJ, 119, 1881
Alencar, S. H. P., & Batalha, C. 2002, ApJ, 571, 378
Arce, H. G., Shepherd, D., Gueth, F., Lee, C.-F., Bachiller, R., Rosen, A., & Beuther, H. 2007, in Protostars and Planets V, ed. B. Reipurth, D. Jewitt, & K. Keil (Tucson: Univ. Arizona Press), in press
Athay, R. G. 1965, ApJ, 142, 755
Avrett, E. H., Vernazza, J. E., & Linsky, J. L. 1976, ApJ, 207, L199
Bally, J., Feigelson, E., & Reipurth, B. 2003, ApJ, 584, 843
Bally, J., & Reipurth, B. 2001, ApJ, 546, 299
Bally, J., Reipurth, B., & Davis, C. J. 2007, in Protostars and Planets V, ed. B. Reipurth, D. Jewitt, & K. Keil (Tucson: Univ. Arizona Press), in press
Beristain, G., Edwards, S., & Kwan, J. 2001, ApJ, 551, 1037
Burrows, C. J., et al. 1996, ApJ, 473, 437
Calvet, N., Muzerolle, J., Briceno, C., Hernandez, J., Hartmann, L., Saucedo, J. L., & Gordon, K. D. 2004, AJ, 128, 1294
Dupree, A. K., Brickhouse, N. S., Smith, G. H., & Strader, J. 2005, ApJ, 625, L131
Edwards, D., Cabrit, S., Strom, S. E., Heyer, I., Strom, K. S., & Anerdson, E. 1987, ApJ, 321, 473
Edwards, S., Fischer, W., Hillenbrand, L., & Kwan, J. 2006, ApJ, 646, 319
Edwards, S., Fischer, W., Kwan, J., Hillenbrand, L., & Dupree, A. K. 2003, ApJ, 599, L41
Favata, F., Fridlund, C. V. M., Micela, G., Sciortino, S., & Kaas, A. A. 2002, A&A, 386, 204
Feigelson, E. D., Broos, P., Gaffney, J. A., III, Garmire, G., Hillenbrand, L. A., Pravdo, S. H., Townsley, L., & Tsuboi, Y. 2002, ApJ, 574, 258
Font, A. S., McCarthy, I. G., Johnstone, D., & Ballantyne, D. R. 2004, ApJ, 607, 890
Gómez de Castro, A. I., & Verdugo, E. 2001, ApJ, 548, 976
Gueth, F., & Guilloteau, S. 1999, A&A, 343, 571
Hamann, F. 1994, ApJS, 93, 485
Hartigan, P., Morse, J. A., Tumlinson, J., Raymond, J., & Heathcote, S. 1999, ApJ, 512, 901
Heasley, J. N., Mihalas, D., & Poland, A. I. 1974, ApJ, 192, 181
Herczeg, G. J., Linsky, J. L., Valenti, J. A., Johns-Krull, C. M., & Wood, B. E. 2002, ApJ, 572, 310
Herczeg, G. J., Wood, B. E., Linsky, J. L., Valenti, J. A., & Johns-Krull, C. M. 2004, ApJ, 607, 369
Herczeg, G. J., et al. 2005, AJ, 129, 2777
Johns-Krull, C. M., & Valenti, J. A. 2001, ApJ, 561, 1060
Johns-Krull, C. M., Valenti, J. A., & Linsky, J. L. 2000, ApJ, 539, 815
Kastner, J. H., Huenemoerder, D. P., Schulz, N. S., Canizares, C. R., & Weintraub, D. A. 2002, ApJ, 567, 434
Königl, A., & Pudritz, R. E. 2000, in Protostars and Planets IV, ed. V. Mannings, A. P. Boss, & S. S. Russell (Tucson: Univ. Arizona Press), 759
Kurucz, R. L., & Bell, B. 1995, CD-ROM 23, Atomic Line Data (Cambridge: SAO)
Lamzin, S. A., Kravtsova, A. S., Romanova, M. M., & Batalha, C. 2004, Astron. Lett., 30, 413
Matsuyama, I., Johnstone, D., & Hartmann, L. 2003, ApJ, 582, 893
Moos, H. W., et al. 2000, ApJ, 538, L1
Mundt, R. 1984, ApJ, 280, 749
Pravdo, S. H., Feigelson, E. D., Garmire, G., Maeda, Y., Tsuboi, Y., & Bally, J. 2001, Nature, 413, 708
Pudritz, R. E., Pelletier, G., & Gomez de Castro, A. I. 1991, in The Physics of Star Formation and Early Stellar Evolution, ed. C. J. Lada & N. D. Kylafis (NATO ASI Ser. C, 342; Dordrecht: Kluwer), 539
Ray, T. P., Mundt, R., Dyson, J. E., Falle, S. A. E. G., & Raga, A. C. 1996, ApJ, 468, L103
Reipurth, B., Bally, J., Fesen, R. A., & Devine, D. 1998, Nature, 396, 343
Reipurth, B., Pedrosa, A., & Lago, M. T. V. T. 1996, A&AS, 120, 229
Reipurth, B., Yu, K. C., Heathcote, S., Bally, J., & Rodríguez, L. F. 2000, AJ, 120, 1449
Roberge, A., et al. 2001, ApJ, 551, L97
Shang, H., Glassgold, A. E., Shu, F. H., & Lizano, S. 2002, ApJ, 564, 853
Shang, H., Li, Z.-Y., & Hirano, N. 2007, in Protostars and Planets V, ed. B. Reipurth, D. Jewitt, & K. Keil (Tucson: Univ. Arizona Press), in press
Shu, F. H., Najita, J., Ostriker, E., Wilkin, F., Ruden, S., & Lizano, S. 1994, ApJ, 429, 781
Shu, F. H., Najita, J. R., Shang, H., & Li, Z.-Y. 2000, in Protostars and Planets IV, ed. V. Mannings, A. P. Boss, & S. S. Russell (Tucson: Univ. Arizona Press), 789
Stanke, T., McCaughrean, M. J., & Zinnecker, H. 2002, A&A, 392, 239
Takami, M., Chrysostomou, A., Bailey, J., Gledhill, T. M., Tamura, M., & Terada, H. 2002, ApJ, 568, L53
Wahlstrom, C., & Carlsson, M. 1994, ApJ, 433, 417
Walter, F. M., et al. 2003, AJ, 126, 3076
Zirin, H. 1975, ApJ, 199, L63